Geologica Acta, Vol.13, Nº 4, December 2015, 325-334
DOI: 10.1344/GeologicaActa2015.13.4.5

geologica acta

LA-MC-ICP-MS dating of zircon from chromitite of the Archean Bangur Gabbro Complex, Orissa, India – Ambiguities and constraints

P.V. SUNDER-RAJU[1, 2] E. HANSKI[2] Y. LAHAYE[3]

[1]**National Geophysical Research Institute (CSIR)**
Uppal Road, Hyderabad, Telangana, India. Raju E-mail.perumala.raju@gmail.com

[2]**Oulu Mining School**
P.O. Box 3000, 90014 University of Oulu, Finland

[3]**Geological Survey of Finland**
P.O. Box 96, 02151 Espoo, Finland

ABSTRACT

The Mesoarchean chromitites in the Singhbhum craton provide the main source of chromium in India. We report here results of dating zircon grains that were found in the chromitite of ultramafic rocks belonging to the southern part of the Archean Baula Complex. The chromite-bearing ultramafic rocks are cut by a gabbronorite intrusion, which had earlier been dated by SHRIMP at 3.12Ga. We have performed isotopic analysis of the zircon grains by Laser Ablation Multicollector Inductively Coupled Plasma Mass Spectrometry (LA-MC-ICP-MS) and obtained an age of 2.84Ga, which is inconsistent with the previous age reported for the gabbronorite. We have also determined the Pb isotopic composition of galena found in the chromitite and found out it was highly radiogenic given the Archean age of its host rock. We discuss the potential reasons for these results, such as later Neoarchean or even Proterozoic tectono-magmatic/hydrothermal events, and stress the importance of future detailed petrographic, mineralogical and isotopic studies to solve the dilemmas.

KEYWORDS **Chromitite. Zircon. Galena. U-Pb isotopes. Pb-Pb isotopes. Archean. Orissa (India).**

INTRODUCTION

Chromite-bearing ultramafic rocks are found in lower parts of mafic-ultramafic layered intrusions and in ophiolitic mantle tectonites (*e.g.*, Stowe, 1987). Chromitites in these environments provide important research targets for studying the petrogenesis of their host rocks, decipher the geotectonic environment of ultramafic rocks and explore metallic resources such as chromium (Cr) and Platinum-Group Elements (PGE). Moreover, chromite is one of the most important minerals for the application of the Re-Os method to mafic-ultramafic complexes, allowing to determine precise initial isotopic ratios (*e.g.*, Puchtel *et al.*, 2001), estimate the degree of crustal contamination in ore-bearing systems (*e.g.*, Walker *et al.*, 1997) and assess the evolution of both the subcontinental lithospheric and convective mantle (Nägler *et al.*, 1997; Walker *et al.*, 2002).

Recognition of ancient ophiolitic complexes is crucial in attempting to constrain the time when plate tectonic processes began on Earth. Ancient ophiolitic complexes are often highly deformed and altered, and their dismembered parts, such as separate pillow lava successions or ultramafic rock lenses, if occurring alone, may lose their potential to witness an ophiolitic origin. However, if chromitites are present in ultramafic rocks, they could potentially be used to track the age and geotectonic setting of ultramafic rocks, because i) chromitites can be well-preserved even though their host rocks are totally altered (*e.g.*, Vuollo *et al.*, 1995; Gornostaev *et al.*, 2004), ii) major and minor element compositions of chromite show variation between different tectonic environments, iii) Os isotopic model ages can be utilized to distinguish Proterozoic and Archean chromitites from each other (*e.g.*, Gornostaev *et al.*, 2004), and iv) initial Os isotopic compositions may be used to distinguish asthenospheric mantle versus old lithospheric mantle as the potential source of the host ultramafic rocks (*e.g.*, Tsuru *et al.*, 2000).

So far, the number of reported occurrences of Archean massive chromitites is limited (*e.g.*, Rollinson, 1997; Rollinson *et al.*, 2002; Gornostaev *et al.*, 2004; Coggon *et al.*, 2013). There are several chromitite occurrences in the Indian Shield, associated with anorthositic complexes (Dharma Rao *et al.*, 2014) or ultramafic-mafic complexes. The latter include sill-like chromitite-bearing layered ultramafic-mafic bodies in the Western Dharwar Craton, southern India (Mukherjee *et al.*, 2012) and the Nuasahi, Sukinda and Jojohatu massifs in the Singhbhum Craton, eastern India (Mondal *et al.*, 2006; Pal *et al.*, 2008). The Mesoarchean Nuasahi and Sukinda massifs host ca. 98% of the total chromite resources of India (Mondal *et al.*, 2006).

The two prominent active chromite mines, Bangur and Baula, occurring in the Nuasahi area in Orissa, were sampled to assess the PGE potential of the area. While studying the chromitites with Field Emission Scanning Electron Microscopy (FESEM), the authors discovered several zircon and galena grains in the samples. In this work, we applied Laser Ablation Multicollector Inductively Coupled Plasma Mass Spectrometry (LA-MC-ICP-MS) to obtain the age for the zircon grains. So far, no dates on the chromitite-bearing ultramafic massifs have been available, although three gabbroic samples belonging to the main Bangur Gabbro intrusion, the upper part of which appears to brecciate chromitite-bearing ultramafic rocks, had earlier been dated at ca. 3.12Ga by the Sensitive High Resolution Ion Microprobe (SHRIMP) method (Augé *et al.*, 2003), thus providing a tentative minimum age for the ultramafic rocks. Our direct LA-MC-ICP-MS analyses of zircon in chromitites, reported in this article, appear to give different results.

GEOLOGICAL BACKGROUND

The eastern part of the Indian Shield is composed of a high-grade metamorphic terrain known as the Chhotanagpur Craton in the north and a granite-greenstone terrain known as the Singhbum Craton in the south. The latter is mainly composed of several granitoid batholiths, which are largely surrounded and intervened by supracrustal rocks.

The Singhbhum terrane is an oval-shaped nucleus with Archean rocks engulfed by Proterozoic rocks towards both the north and south (Saha, 1994). In the eastern part of the Indian subcontinent, the Precambrian crust evolved by accretion of younger terranes around this complex. The main lithological units of Singhbhum include an Older Metamorphic Group (OMG), the granite massifs of Singhbhum, Bonai and Kaptipada, and the Pallahara granite gneiss, with younger supracrustals comprising iron ores. The Iron Ore Group (IOG) rocks are present within the Kolhan basin and towards the boundary of the Singhbhum granite massifs. The IOG rocks were also termed greenstone belts by Acharyya (1993). Unlike the other supracrustals belts, earlier reports described the Singhbhum craton as devoid of komatiitic rocks. However, recent studies by Chaudhri *et al.* (2015) report both textural and mineralogical evidence for the presence of Mesoarchean Barberton-type komatiites in the eastern IOG. The Ar/Ar data indicate that the OMG rocks were affected by the intrusion of Singhbhum granites before 3300 Ma and cooled below ~500ºC at ~3.3Ga. The OMG rocks were are also intruded by older tonalite to granodiorite intrusions, presently known as metamorphic tonalitic gneisses (OMTG) that have provided U-Pb zircon intrusion ages of ~3.4Ga and ~3.2Ga (Mishra *et al.*, 1999). The ~3.4Ga event is interpreted as the time of formation of the protoliths of the OMTG while the ~3.2Ga age is regarded as a metamorphic event that overprinted both the OMG and OMTG. The measured ages were corroborated by Rb-Sr whole rock isochron dates by Basu *et al.* (2008). Finally, Mukhopadhyay *et al.* (2008) have reported a zircon U-Pb age of 3.51Ga for dacitic lava in an IOG supracrustal sequence belonging to Tomako-Daitari greenstone belts, while Basu *et al.* (2008) published a 3.4Ga zircon U-Pb age from volcanic rocks belonging to the western IOG. Thus, taking into account the available information, it appears that the age of the ultramafic-mafic magmatism falls in the range of 3.09-2.5Ga. Encircling the southeastern fringe of the Singhbhum Craton, ultramafic bodies stretch from Niligiris in the northeast through Baula and Sukinda to Deogarh in the Southwest. They also intrude into the Eastern Ghat Mobile Belts (EGMB). The Baula-Nuasahi Ultramafic Complex (BNUC; lat. 21º.15'–21º.20'; long. 86º.18'–86º.20') is located approximately **5**0km NE of the Sukinda Ultramafic belt.

GEOLOGY OF THE BAULA COMPLEX AND PREVIOUS ISOTOPIC WORK

The Baula-Nuasahi Ultramafic Complex (BNUC) is intrusive into a clastic-dominated metavolcanosedimentary suite of rocks belonging to the Badampahar-Gorumhisani Group of Iron Ore Supergroup (IOSG). This lithological sequence, which is locally called the Hadgarh Group, has undergone greenschist facies metamorphism and multiphase deformation. The BNUC extends in a NNW-SSE direction over a strike length of 3.5km and 1.5km width at the center, gradually tapering towards both the north and south. The southern part of the Baula Complex includes three main units, viz. the Chromitite-bearing Ultramafic Rock unit, the Gabbro–Anorthosite unit and the intrusive Bangur Gabbro (Fig. 1). The Bangur Gabbro is a gabbronorite with a porphyritic texture, which locally cuts and incorporates dunite with chromitite layers as inclusions. The Bangur Gabbro also cuts the Gabbro–Anorthosite unit giving rise to a magmatic breccia. The breccia zone is 1-40 m thick and has a strike length of ca. 2Km (Augé *et al.*, 2003). The matrix is predominantly gabbro and plagioclase-bearing pyroxenite that correspond to the rock types of the Bangur Gabbro (Fig. 2C, D).

The Bangur chrome mine is located in the southern part of the belt, which is cut across by a coarse- to medium-grained pegmatitic variety of gabbro. In general, the chromitite seams show variable textural forms, such as disseminated, massive, schlieren, banded chromite and clot textures (Fig. 2B). The chromite grains are variably altered to ferritchromite.

Using the SHRIMP technique, a zircon U-Pb age of 3122±5Ma was obtained by Augé *et al.* (2003) for the pegmatoid gabbro-norite of the Bangur Gabbro. The gabbro-norite was interpreted as intrusive in chromitites of the Bangur open pit and thus would give a minimum age for the chromitite, whereas similar ages (3123±7Ma, 3119±6Ma) were obtained by the same authors in two other gabbroic samples from the Baula Complex.

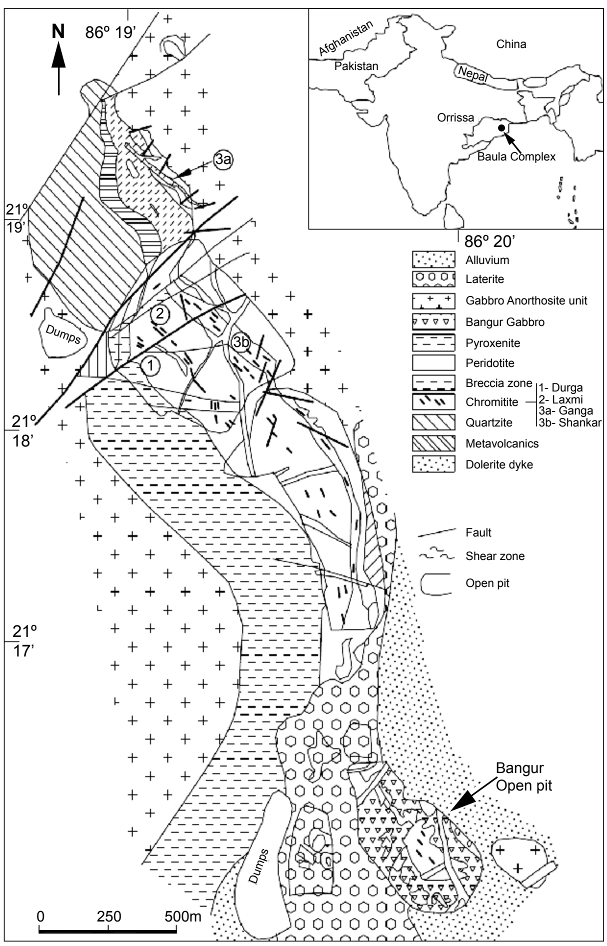

FIGURE 1. Geological Map of Bangur open pit (after Geological Survey of India, BRGM, India).

PETROGRAPHY AND MINERALOGY OF STUDIED SAMPLES

Epoxy mounts of the chromitite samples (Fig. 3) were prepared and studied for their petrography and mineralogy. The samples consist mostly of chromite crystals, which were originally commonly euhedral but are now often fractured or brecciated and locally transformed into a fine-grained assemblage of small angular fragments (Fig. 4A, B). In transmitted light, they are brownish red indicating that they are not altered. This is also evident in reflected light showing no zoning to more light-colored, Fe^{3+}-richer domains.

Augé *et al.* (2003) and Mondal *et al.* (2007) reported the presence of various PGE minerals in the sulfur-rich and sulfur-poor zones of the Bangur chromitites, including sperrylite, merenskyite, braggite, isoferroplatinum and ruarsite. The capability of FESEM was utilized to analyze Platinum Group Minerals (PGMs) with a size down to 0.2 microns with a reasonable accuracy. In addition to PGMs, these studies on chromitite samples revealed the presence of unusual rare and exotic minerals such as zircon, galena, antimony, and millerite. Zircon is irregularly distributed in the chromitite samples. The grain size of zircon grains is small, with the maximum observed diameter being ca. 50 microns. However, the number of grains is relatively large, for example in four polished mounts tens of grains were found. Individual zircon grains (Fig. 4C) occur mostly in the silicate matrix and are aligned roughly parallel to the chromite bands. Most of the grains are subhedral to anhedral with no clear zoning. It is noteworthy that zircon grains may contain chromite inclusions. In six polished mounts, ca. 10 zircon grains were found that contain chromite inclusions up to >20 microns in size.

Galena mainly occurs in the chromite grains and in secondary silicates in minute amounts, with their grain size ranging from 3 to 40 microns (Fig. 4D). The galena contains 86.2 to 88.6wt% Pb with minor amounts of Fe up to 0.30wt%, but no measurable Sb or Bi.

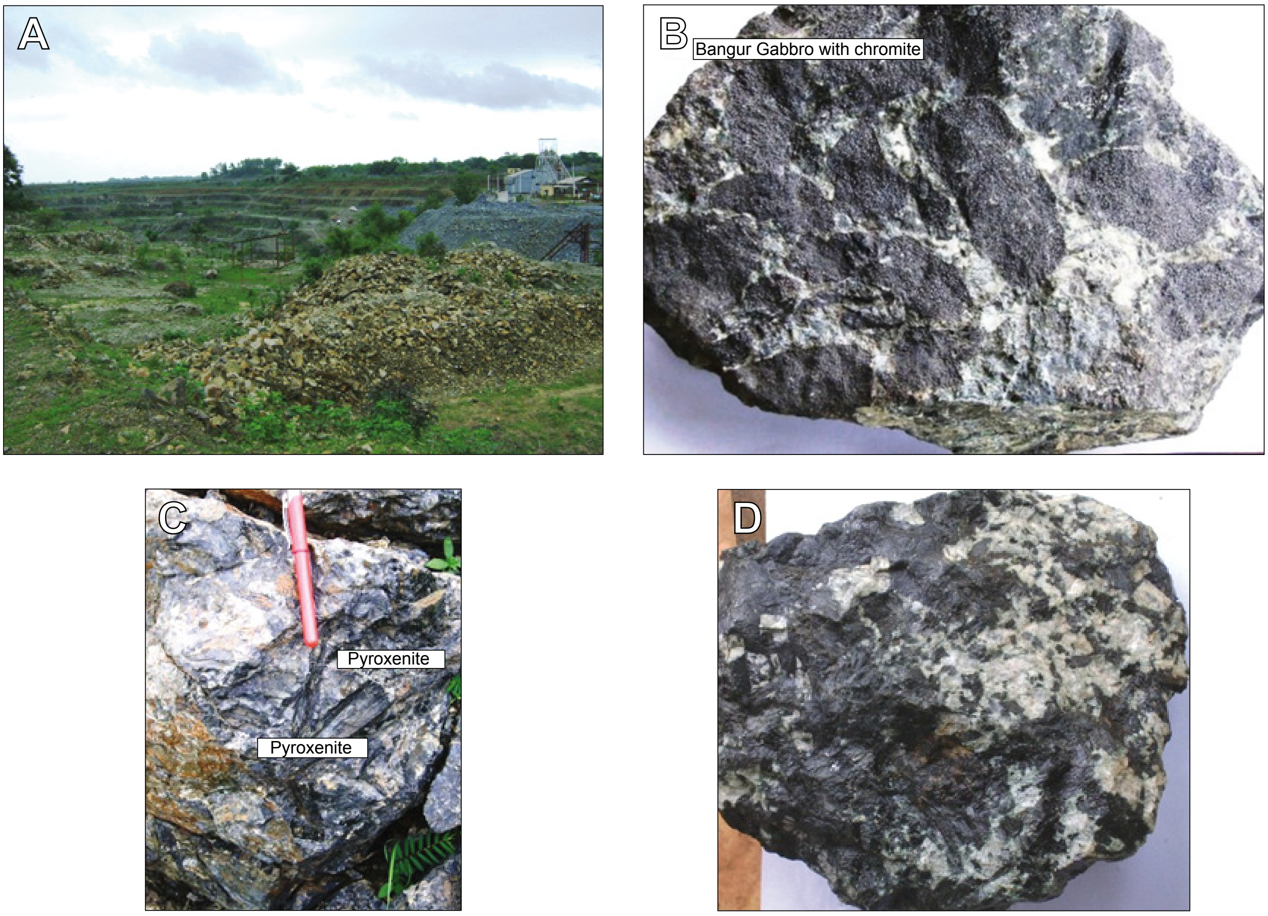

FIGURE 2. A) Overview of the Bangur chromite pit. B) Bangur Gabbro with brecciated chromite. C) Pyroxenite laths in Bangur gabbro. D) Brecciated Gabbro with sulphides.

ANALYTICAL METHODS

U-Pb isotopic analyses of zircons were mounted in epoxy and of the chromitite samples (Fig. 3) were performed using a Nu Plasma HR Multicollector ICP-MS coupled to a Photon Machine Analyte G2 laser microprobe at the Geological Survey of Finland in Espoo. The technique is very similar to that published by Rosa *et al.* (2009). Samples were ablated in Helium (He) gas (gas flows=0.4 and 0.1l/min) within a HelEx ablation cell (Müller *et al.*, 2009). The He aerosol was mixed with Argon (Ar) (gas flow=0.8l/min) prior to entry into the plasma. All analyses were carried out in static ablation mode under normal conditions, such as 20µm beam diameter, 5Hz pulse frequency and 0.55J/cm^2 beam energy density. A single U–Pb measurement included 30s of on-mass background measurement, followed by 60s of ablation with a stationary beam. Masses 204, 206 and 207 were measured in secondary electron multipliers, and 238 in an extra high mass Faraday collector. ^{235}U was calculated from the signal at mass 238 using a natural ^{238}U/^{235}U=137.88. Mass number 204 was used as a monitor for common ^{204}Pb after discarding the ^{204}Hg background. In an ICP-MS analysis, ^{204}Hg mainly originates from the He supply. The observed background counting-rate on mass 204 was ca. 1200 (ca. 1.3×10^{-5}V), and has been stable at that level over the last year. The contribution of ^{204}Hg from the plasma was eliminated by on-mass background measurement prior to each analysis. Age-related common lead (Stacey and Kramers, 1975) correction was used when the analysis showed common lead contents above the detection limit. Signal strengths on mass 206 were typically >10^{-3}V, depending on the uranium content and age of the zircon. Two calibration standards were run in duplicate at the beginning and end of each analytical session, and at regular intervals during sessions. Raw data were corrected for the background, laser-induced elemental fractionation, mass discrimination and drift in ion counter gains and reduced to U-Pb isotope ratios by calibration to concordant reference zircons of known age, using protocols adapted from Andersen *et al.* (2004) and Jackson *et al.* (2004). Standard zircons GJ-01 (609±1Ma; Belousova *et al.*, 2006) and an in-house standard A1772 (2712±1Ma, Huhma *et al.*, 2012) were used for calibration. The calculations were performed off-line, using an interactive spreadsheet program written in Microsoft Excel/VBA by T. Andersen (Rosa *et al.*, 2009). To minimize the effects of laser-induced elemental fractionation, the depth-to-diameter ratio of the ablation pit was kept low, and isotopically homogeneous segments of the time-resolved traces were calibrated against the corresponding time interval for each mass in the reference zircon. To compensate for drift in instrument sensitivity and Faraday vs. electron multiplier gain during an analytical session, a correlation of signal vs. time was assumed for the reference zircons. A description of the algorithms used is provided in Rosa *et al.* (2009). Plotting of the U-Pb isotopic data and age calculations were performed using the Isoplot/Ex 3 program (Ludwig, 2003). All the ages were calculated with 2σ errors and without decay constants errors. Data-point error ellipses in the figures are at the 2σ level. The concordant age offset from ID-TIMS ages for several samples of quality control including zircon 91500 (1066Ma) and A382 (1877±2Ma; Patchett and Kouvo, 1986; Huhma *et al.*, 2012) does not exceed 0.5%.

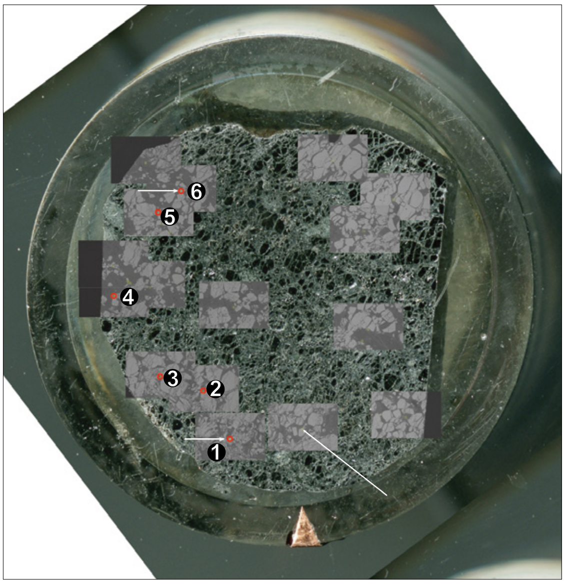

FIGURE 3. Sample 8-OM with analysis spots in 1" polished epoxy button.

RESULTS

U-Pb and Pb-Pb isotope analyses

An epoxy-mounted polished button of chromitite sample 8-OM contained more than 50 zircon grains (Fig. 3). Four grains were large enough for analysis using the 20µm spot size. One to three analyses were performed on each grain. The analytical results are presented in Table 1. As shown in Figure 4, there is a homogeneous zircon population in this sample, with all the measured compositions plotting at or close to the Concordia curve. They give a mean age of 2835±8Ma (2σ), which is almost 300Ma younger that the previously published Mesoarchean ages of the Bangur Gabbro. A galena grain was analysed for lead isotopes. Measured isotopic ratios with 2σ errors are the following $^{206}Pb/^{204}Pb$=16.552±0.007, $^{207}Pb/^{204}Pb$=15.361±0.008, $^{208}Pb/^{204}Pb$=36.865±0.020. Because the post-crystallization ingrowth of radiogenic Pb is insignificant in galenas, we can take these ratios as the initial values at the time of galena formation.

DISCUSSION

Zircon is a mineral that is commonly utilized for dating mafic to felsic igneous rocks, but rarely occurs, or is not abundant enough, in chromitites and their host ultramafic rocks to allow their dating using conventional separation and Isotope Dilution-Thermal Ionization Mass Spectrometry (ID-TIMS) methods. One exception was provided by Grieco *et al.* (2001) who reported a zircon U-Pb age of ca. 210Ma for chromitite-bearing dunites associated with a phlogopite peridotite mantle slab in the Ivrea Zone, Southern Alps. This age is around 340Ma younger than that of the peridotite and is interpreted as the time of mantle metasomatism caused by injection of phlogopite-bearing pyroxenite dikes into the peridotite.

The presence of exotic minerals like zircon or galena in chromitites has been reported earlier. Zircon as individual grains in the matrix with chromite and silicates was found for instance in the Finero Ultramafic Complex in Italy, (Grieco, 1998). Small zircon grains in chromites have also been documented from typical layered intrusions, such as the Bushveld Complex (Iain *et al.*, 2005), Plat-Reef (Merkle, 1992), UG-2 and Merensky Reef (Zaccarini *et al.*, 2004; Irvine, 1977) in South Africa. Also, galena is present as inclusions in chromite grains of the Kemi intrusion in Finland (Alapieti *et al.*, 1990) and Campo Formoso in Brazil (Zaccarini *et al.*, 2006). The studies carried out on sulfur fugacity as a function of temperature by Barton and Skinner (1978) demonstrated that galena needs higher fS_2 than that needed to form pyrrhotite. It is, therefore, not likely that it forms before this mineral. The slope of the buffer lines indicates that at increasing temperature (*i.e.* magmatic conditions) the difference will become larger and no crossover (*i.e.* galena becomes stable at lower fS_2 than pyrrhotite) will occur. Galena melts congruently at 1127±5ºC and pyrrhotite at 1190ºC. When an immiscible sulfur melt forms, the much more common iron in the basaltic silicate melt will grab the sulfur before lead could do it. This strongly supports the hypothesis that the galena grains were formed by hydrothermal processes or, as Irvine (1977) reported, that these types of inclusions may also represent droplets of trapped liquid from contaminant sialic melt. This has also been confirmed by recent studies (Burton *et al.*, 2012) that suggest that these kinds of inclusions may also form due to specific chemical

TABLE 1. LA-MC-ICPMS analyses on zircon

Name	ppm U	ppm ^{206}Pb	$^{206}Pb_c$(%)	Ratios $^{206}Pb/^{204}Pb$	$^{207}Pb/^{206}Pb^*$	1s	$^{207}Pb/^{235}U$	1s	$^{206}Pb/^{238}U$	1s	Rho	Discordance Central (%)	Ages & 1s errors (Ma) $^{207}Pb/^{206}Pb$	1s	$^{207}Pb/^{235}U$	1s	$^{206}Pb/^{238}U$	1s
Quality control standard: A382																		
A382-1	258	114.8	0.00E+00	30923	0.11393	0.00058	5.43746	0.10485	0.34614	0.00644	0.964	3.3	1863	9	1891	17	1916	31
A382-2	148	65.4	0.00E+00	15247	0.11402	0.0006	5.30167	0.10059	0.33723	0.00615	0.961	0.5	1864	9	1869	16	1873	30
A382-3	438	193.6	0.00E+00	22724	0.11373	0.00074	5.35486	0.1916	0.34148	0.01202	0.983	2.1	1860	11	1878	31	1894	58
A382-4	133	60.1	0.00E+00	5215	0.11435	0.00065	5.52415	0.14162	0.35038	0.00876	0.975	4.1	1870	10	1904	22	1936	42
A382-5	134	59.5	0.00E+00	24084	0.11487	0.00076	5.4882	0.14369	0.34651	0.00878	0.967	2.5	1878	12	1899	22	1918	42
A382-6	238	101	0.00E+00	35883	0.11392	0.00062	5.34403	0.11794	0.34022	0.00728	0.969	1.5	1863	10	1876	19	1888	35
A382-7	112	50.6	0.00E+00	8865	0.11489	0.00075	5.54437	0.16894	0.35	0.01042	0.977	3.5	1878	12	1908	26	1935	50
Samples																		
OM8-4a	105	73.1	0.00E+00	11124	0.20139	0.0013	14.5548	0.32522	0.52416	0.01121	0.957	-5.2	2838	10	2787	21	2717	47
OM8-4b	84	63.1	0.00E+00	4430	0.20078	0.00131	15.7084	0.37867	0.56742	0.01317	0.963	2.8	2833	10	2859	23	2897	54
OM8-5a	65	48	8.40E-03	8057	0.20135	0.00132	15.7256	0.40392	0.56643	0.01407	0.967	2.4	2837	10	2860	25	2893	58
OM8-6a	122	88.8	0.00E+00	18756	0.20102	0.00137	15.3092	0.37654	0.55236	0.01306	0.961 .		2834	11	2835	23	2835	54
OM8-6b	59	46.3	0.00E+00	7081	0.20121	0.00141	15.9778	0.50348	0.57592	0.01769	0.975	4.2	2836	11	2875	30	2932	72
OM8-6c	131	97.1	0.00E+00	18103	0.20087	0.00128	15.125	0.34629	0.54611	0.01201	0.961	-1.1	2833	10	2823	22	2809	50
OM8-7a	62	47.4	0.00E+00	9242	0.20178	0.00156	15.6918	0.59847	0.56401	0.02106	0.979	1.9	2841	12	2858	36	2883	87

reactions between anhydrous silicates from the chromite-precipitating magma (olivine and pyroxene) and trapped volatile-rich silicate melt and fluids occurring inside the inclusions.

Our study shows that methods, such as LA-MC-ICP-MS, can be used to date tiny zircon crystals in ultramafic rocks. Yet, the U-Pb age of 2836±8Ma, (Fig. 5) measured in this work for the zircons occurring in the Bangur chromitite is ca. 300 younger than the U-Pb zircon age obtained by Augé *et al*. (2003) by the SHRIMP methods for a pegmatoid gabbro-norite intrusion interpreted as cutting the chromitite. This is contrary to what would be expected if the zircon grains in the chromitite represent the

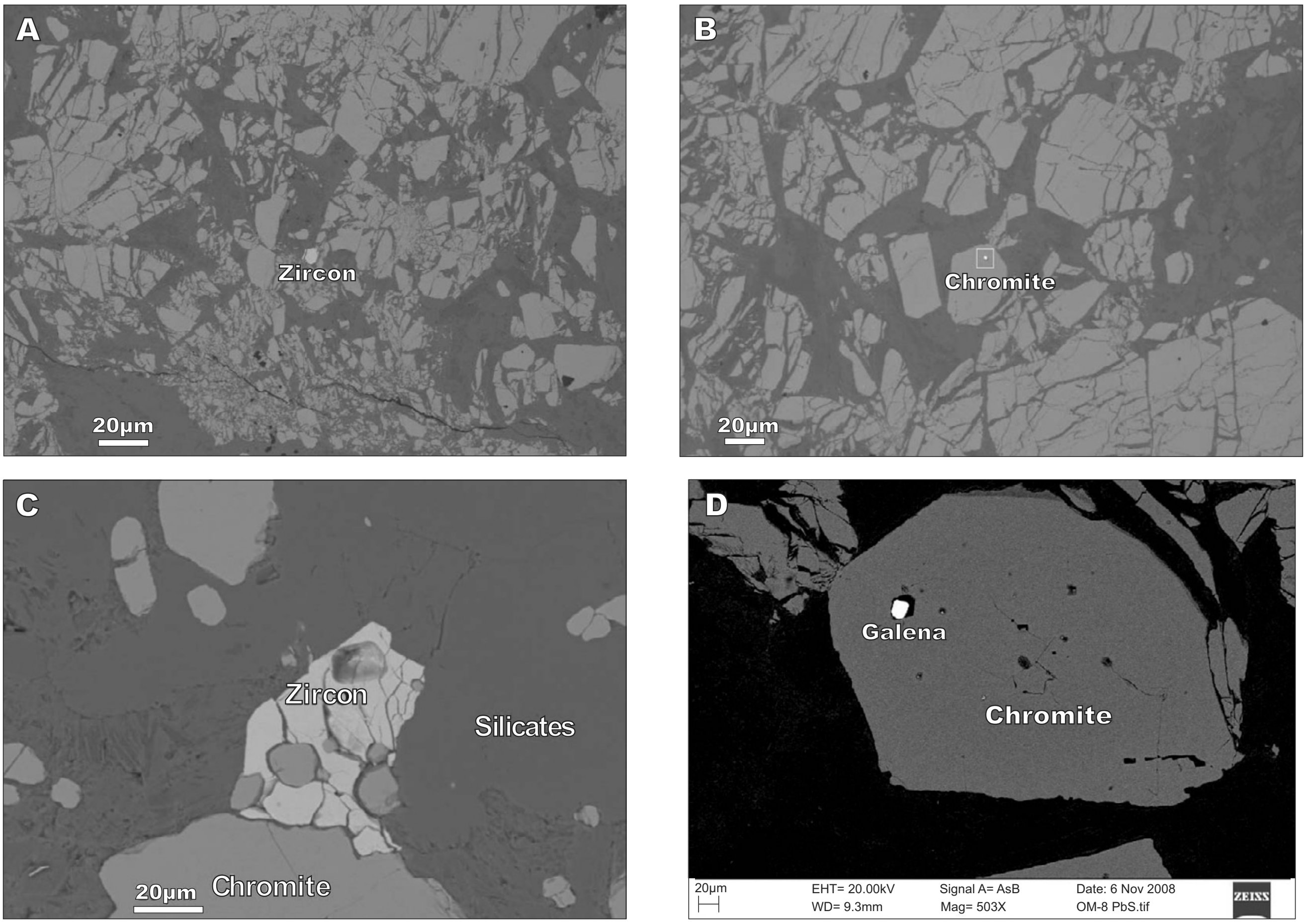

FIGURE 4. Back-scattered electron images of chromitite samples. A) Fractured euhedral chromite grains. B) Zircon grain in chromite. C) Zircon with chromite inclusions. D) Galena inclusion in chromite grain enlarged from B.

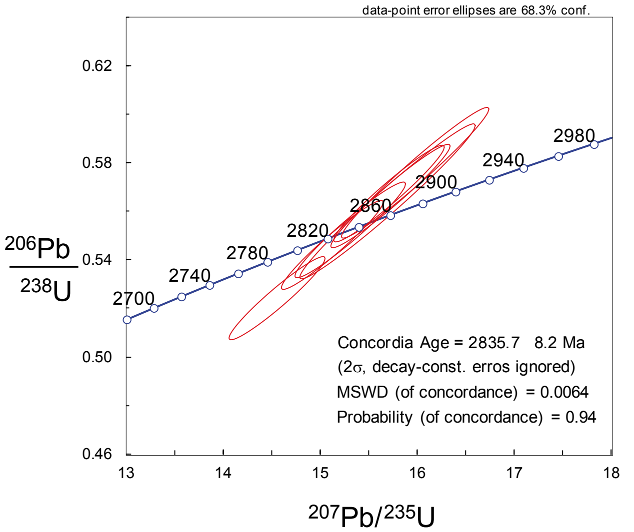

FIGURE 5. Condoria diagram of insitu LA-ICP-MS analyses of zircon grains from Bangur chromitite.

age of their host rock. In our opinion, the paradoxical age relationship now disclosed can be explained by two ways. Either the age published by Augé *et al.* (2003) does not record the age of the Bangur Gabbro but that of inherited zircon, or the zircon studied in this study is younger than the age of the chromite and was generated by later hydrothermal processes. The first option seems unlikely because inherited zircons are more common in low-T felsic magmas than in high-T mafic magmas. Moreover, Augé *et al.* (2003) obtained similar ca. 3.22Ga ages for three separate gabbroic samples from the area. The hydrothermal origin, instead, is compatible with the mode of occurrence of the zircon in the silicate matrix of the chromitite and with its morphology and homogeneous nature. If so, the zircon likely represents the timing of the brecciation of the chromitite.

The geochemical studies of trace elements by Mondal and Zhou (2010) suggest that metasomatism played a significant role within the breccia portion by evolved boninitic melt. The entire package was later reworked by hydrothermal alteration due to interaction of sea water (Mondal *et al.*, 2003).

The obtained lead isotope composition of the galena grain is shown in a $^{206}Pb/^{204}Pb$ vs. $^{207}Pb/^{204}Pb$ diagram in Figure 6 together with the model Pb isotope evolutions of the upper mantle and upper crust of Kramers and Tolstikhin (1997). The galena composition plots below but not far from the mantle curve. However, it is close to the ca. 1.2Ga mantle composition and hence much more radiogenic than the composition of the Archean mantle. For example, compared with the measured $^{206}Pb/^{204}Pb$ ratio of 16.6, the upper mantle has an unradiogenic $^{206}Pb/^{204}Pb$ ratio of ca. 13.5 at 2.8Ga and an even more unradiogenic ratio of ca. 12.5 at 3.2Ga. This rules out a direct formation of the lead in galena from a Mesoarchean mantle-derived magma. Furthermore, the initial Os isotope composition of the Bangur chromitites is unradiogenic, yielding negative γOs values in the range of -0.90 to -2.64 as calculated at 3.2Ga (Mondal, 2007). Hence, if the galena was coeval with the chromitites and was produced by magmatic processes, an unradiogenic Pb composition should also be expected for it (*cf.* Burton *et al.*, 2012), which is in stark contrast to what has been measured.

Assuming that the galena grain has the same age as the associated zircon grains, a 2835Ma isochron was drawn through the galena composition in Figure 6. This isochron intersects the upper crustal Pb isotopic evolution curve at ca. 3300Ma, which suggests that the lead has an ancient crustal source. One potential scenario is that a crustal source generated a partial melt at ca. 3300Ma, crystallizing into a rock that had a sufficiently high μ ($^{238}U/^{204}Pb$) to develop a radiogenic Pb isotope composition within the next 400Ma. Partial melting of this rock produced a melt from which the galena crystallized and registered its isotopic composition. However, to fulfill this model, the μ value needs to be higher than 50.

A third option is that the galena has an age that is much younger than that of the zircon, *e.g.* around 1.0-1.5Ga, which would make its radiogenic Pb isotopic composition easier to interpret. However, this would mean that the rocks were affected by two thermal events after their generation at ca. >3120Ma, one at ca. 2835Ma recorded by hydrothermal zircon and the other in the Proterozoic time recorded by galena. The latter event could be linked to the

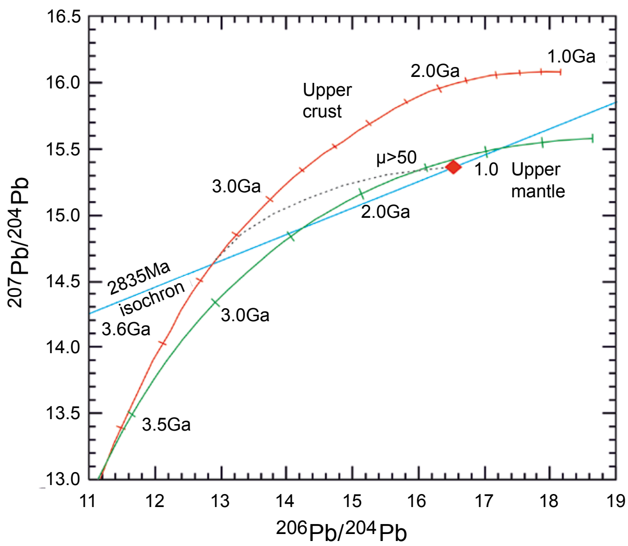

FIGURE 6. $^{206}Pb/^{204}Pb$ vs. $^{207}Pb/^{204}Pb$ diagram showing the measured galena composition together with model upper mantle and upper crust Pb isotopic evolution curves after Kramers and Tolstikhin (1997).

Mesoproterozoic magmatism that has been recognized to have taken place in the Singhbhum Craton at ca. 1.5–1.6Ga (Chatterjee *et al.*, 2013; Meert and Pandit, 2015). However, any model suggesting post-3.12Ga formation of the galena is inconsistent with the observation that galena grains seem to occur as inclusions in chromite grains (Fig. 4D). Clearly, more integrated research is vital to elucidate this dilemma.

CONCLUSIONS

i) Using the LA-MC-ICP-MS method, we measured an in situ U-Pb age of 2836±8Ma for small zircon grains occurring in the Bangur chromitite.

ii) The obtained age is almost 300Ma younger that the previously published MesoArchaean age of the Bangur Gabbro.

iii) The Pb isotopic composition of galena found in chromitite is highly radiogenic and close to that of the 1.2Ga mantle compositions.

iv) The isotopic data suggest that the rocks were affected at least by two, so far, not well understood thermal events after their generation.

ACKNOWLEDGMENTS

PVSR gratefully acknowledges the financial support from the Finnish government (CIMO grant) and SHORE, PSCO-205 project by CSIR, India. The authors are grateful for the sage advice of Prof. Fernández-Suárez, an anonymous reviewer and Fernando Bea.

REFERENCES

Acharyya, S.K., 1993. Greenstones from Singhbhum Craton, their Archaean character, oceanic crustal affinity and tectonics. Proceedings of the National Academy of Sciences, India, 63(A), 211-222.

Alapieti, T.T, Filen, B.A, Lahtinen, M.M, Lavrov, M.M, Smolkin, V.F, Voitsekhovsky, S.N., 1990. Early Proterozoic layered intrusions in the Northeastern part of the Fennoscandian Shield. Mineralogy and Petrology, 42, 1-22.

Andersen, T, Griffin, W.L., Jackson, S.E., Knudsen, T.L., Pearson N.J., 2004. Mid-Proterozoic magmatic arc evolution at the southwest margin of the Baltic Shield. Lithos, 73, 289-318.

Augé, T., Cocherie, A., Genna, A., Armstrong, R., Guerrot, C., Mukherjee, M.M., Patra, R.N., 2003. Age of the Baula PGE mineralization (Orissa, India) and its implications concerning the Singhbhum Archaean nucleus. Precambrian Research, 121, 85-101.

Barton, P.B,. Skinner, B.J., 1978. Sulfide mineral stabilities. In: Barnes, H.L. (ed.). Geochemistry of Hydrothermal Ore Deposits. New York, Holt, Rinehart & Winston, 236-233

Basu, A.R., Bandyopadhyaya, P.K., Chakrabarthi, R., Zhou, H., 2008. Large 3.4 Algoma type BIF in the Eastern India craton. Goldschmidt conference, Abstracts, Chemical Geology, 72, A 59.

Belousova, E.A., Griffin, W.L., O'Reilly, S.Y., 2006. Zircon crystal morphology, trace element signatures and Hf isotope composition as a tool for petrogenetic modeling. Examples from Eastern Australian granitoids. Journal of Petrology, 47, 329-353.

Burton, K.W., Cenki-Tok, B., Mokadem, F., Harvey, J., Gannoun, A., Alard, O., Parkinson, I.J., 2012. Unradiogenic lead in Earth's upper mantle. Nature Geoscience, 5, 570-573.

Chatterjee, P., De, S., Ranaivoson, M., Mazumder, R., Arima, M., 2013. A review of the ~1600Ma sedimentation, volcanism, and tectono-thermal events in the Singhbhum craton, Eastern India. Geoscience Frontiers, 4, 277-287.

Chaudhri, T., Mazumder, R., Arima, M., 2015. Petrography and geochemistry of Mesoarchean komatiites from eastern iron ore belt, Singhbhum craton, India and its similarity with Barberton type komatiites. Journal of African Earth Sciences, 101, 135-147.

Coggon, J.A., Luguet, A., Nowell, G.M., Appel, P.W.U., 2013. Hadean mantle melting recorded by southwest Greenland chromitite 186Os signatures. Nature Geoscience, 6, 871-874.

Dharma Rao, C.V., Santosh, M., Tang, Y.-J., 2014. Re-Os isotope systematics of Archean chromitites from the Chimalpahad Anorthosite Complex, south-east India. Implications for mantle extraction processes. Ore Geology Reviews, 65, 274-282.

Gornostaev, S.S., Walker, R.J., Hanski, E., Popovchenko, S.E., 2004. Evidence for the emplacement of ca. 3.0 Ga lithospheric mantle in the Ukrainian Shield. Precambrian Research, 132, 351-364.

Grieco, G., 1998. Chromite and PGE mineralisation of the Finero Complex (Southern Alps, Italy) .relations with metasomatic processes. Plinius, 19, 134-140.

Grieco, G., Ferrario, A., Von Quadt, A., Koeppel, V., Mathez, E.A., 2001,The zircon-bearing chromitites of the phlogopite peridotite of Finero (Ivrea Zone, Southern Alps). Evidence and geochronology of a metasomatized mantle slab. Journal of Petrology, 42,89-101.

Huhma, H., Mänttäri, I., Peltonen, P., Halkoaho, T., Hanski, E., Hokkanen, T., Hölttä, P., Juopperi, H., Konnunaho, J., Kontinen, A., Lahaye, Y., Luukkonen, E., Pietikäinen, K., Pulkkinen, A., Sorjonen-Ward, P., Vaasjoki, M., 2012.The age of the Archean schist belts in Finland. Geological Survey of Finland, 54 (Special Paper), 74-175.

Iain McDonald, A.E., Holwell, D.A., Armitage, P.E.B., 2005. Geochemistry and mineralogy of the Platreef and "Critical Zone" of the northern lobe of the Bushveld Complex, South Africa. Implications for Bushveld stratigraphy and the development of PGE mineralisation. Mineralium Deposita, 40, 526-549.

Irvine, T.N., 1977. Origin of chromitite layers in the Muskox intrusion and other layered intrusions. A new interpretation. Geology, 2, 273-277.

Jackson, S.E., Pearson, N.J., Griffin, W.L., Belousova, E.A., 2004. The application of laser ablation-inductively coupled plasma-mass spectrometry to in-situ U–Pb zircon geochronology. Chemical Geology, 211, 47-69.

Kramers, J.D., Tolstikhin, I.N., 1997. Two terrestrial lead isotope paradoxes, forward transport modelling, core formation and the history of the continental crust. Chemical Geology, 139, 75-110.

Ludwig, K.R., 2003. User's manual for Isoplot/Ex, Version 3.00. A geochronological toolkit for Microsoft Excel. Berkeley Geochronology Center, 4 (Special Publication), 75pp.

Meert, J.G., Pandit, M.K., 2015. The Archean and Proterozoic History of Peninsular India. Tectonic Framework for Precambrian Sedimentary Basins in India. In: Mazumder, R., Eriksson, P.G. (eds.). Precambrian Basins of India: Stratigraphic and Tectonic Context. London, Geological Society, 43 (Memoirs), 29-54. http://dx.doi.org/10.1144/M43.3

Merkle, R.K.W., 1992. Platinum-group minerals in the middle group of chromitite layers at Marikana, western Bushveld Complex –Indications for collection mechanisms and post-magmatic modification. Canadian Journal of Earth Sciences, 29, 209-221.

Mishra, S., Domnarari, M.P., Widenbeck, M., Goswami, J.N., Ray, S., Saha, A.K., 1999. 207Pb/206Pb zircon ages of the evolution of Singhbum craton, eastern India, an ion microprobe study. Precambrian Research, 93, 139-151.

Mondal, S.K., Ripley, E.M., Li, C., Ahmed, A.H., Arai, S., Liipo, J., Stowe, C., 2003. Oxygen isotopic compositions of Cr spinels from Archean to Phanerozoic chromite deposits. Geochimica et Cosmochimica Acta, 185 (Supplementary Volume), A 301.

Mondal, S.K., 2007. PGE distributions in Mesoarchaean chromitites and mafic-ultramafic rocks in the Singhbhum Craton (India). Evidence for presence of a subchondritic source mantle domain. Abstract published in Geochimica et Cosmochimica Acta Goldschmidt Conference 2007. Cologne, Abstracts, 680.

Mondal, S.K., Ripley, E.M., Li, C., Frei, R., 2006. The genesis of Archaean chromitites from the Nuasahi and Sukinda massifs in the Singhbhum Craton, India. Precambrian Research, 148, 45-66.

Mondal, S.K., Frei, R., Ripley, E.M., 2007. Os isotope systematics of Mesoarchaean chromitite-PGE deposits in the Singhbhum Craton (India). Implications for the evolution of lithospheric mantle. Chemical Geology, 244, 391-408.

Mondal, S.K., Zhou, M.-F., 2010. Enrichment of PGE through interaction of evolved boninitic magmas with early formed cumulates in a gabbro-breccia zone of the Mesoarchean Nuasahi Massif (eastern India). Mineralium Deposita, 45, 69-91.

Mukherjee, R., Mondal, S.K., Frei, R., Rosing, M.T., Waight, T.E., Zhong, H., Ravindra Kumar, G.R., 2012. The 3.1 Ga Nuggihalli chromite deposits, Western Dharwar craton (India), geochemical and isotopic constraints on mantle sources, crustal evolution and implications for supercontinent formation and ore mineralization. Lithos, 155, 392-409.

Mukhopadhyay, J., Beukes, N., Armstrong, R.A., Zimmermann, U., Ghosh, G., Medda R.A., 2008. Dating the oldest greenstone in India. A 3.51 Ga precise Pb-Pb SHRIMP zircon age for dacitic lava of southern Iron Ore group Singhbhum Craton. Journal of Geology, 116, 449-461.

Müller, W., Shelley, M., Miller, P., Broude, S., 2009. Initial performance metrics of a new custom-designed ArF excimer LA-ICPMS system coupled to a two-volume laser-ablation cell. Journal of Analytical Atomic Spectrometry, 24, 209-214.

Nägler, T.F., Kramers, J.D., Kamber, B.S., Frei, R., Prendergast, M.D.A., 1997. Growth of subcontinental lithospheric mantle beneath Zimbabwe started at ~3.8 Ga. A Re-Os study on chromites. Geology, 25, 983-986.

Pal, T., Ghosh, B., Chakraborty, S., 2008. Petrogenesis of Archaean chromite deposits of the Roro-Jojohatu area in the Singhbhum Craton. A boninitic parental melt in supra-subduction zone setting. Journal of the Geological Society of India, 72, 635-647.

Patchett, J., Kouvo, O., 1986. Origin of continental crust of 1.9-1.7 Ga age. Nd isotopes and U-Pb zircon ages in the Svecokarelian terrain of south Finland. Contributions to Mineralogy and Petrology, 92, 1-12.

Puchtel, I.S., Brugmann, G.E., Hofmann, A.W., Kulikov, S., Kulikova, V., 2001. Os isotope systematics of komatiitic basalts from the Vetreny belt, Baltic Shield. evidence for a chondritic source of the 2.45 Ga plume. Contributions to Mineralogy and Petrology, 140, 588-599.

Rollinson, H., 1997. The Archaean komatiite-related Inyala chromitite, Southern Zimbabwe. Economic Geology, 92, 98-107.

Rollinson, H., Appel, P.W.U., Frei, R., 2002. A metamorphosed, early Archaean chromitite from West Greenland. Implications for the genesis of Archaean anorthositic chromitites. Journal of Petrology, 43, 2143-2170.

Rosa, D.R.N., Finch, A.A., Andersen, T., Inverno, C.M.C., 2009. U-Pb geochronology and Hf isotope ratios of magmatic zircons from the Iberian pyrite belt. Mineralogy and Petrology, 95, 47-69.

Saha, A.K., 1994. Crustal evolution of Singhbum, North Orissa, eastern India. Bangalore, Geological Society of India, 27 (Memoir), 341pp.

Stacey, J.S., Kramers, J.D., 1975. Approximation of terrestrial lead isotope evolution by a two-stage model. Earth and Planetary Science Letters, 26, 207-221.

Stowe, C.W. (ed.), 1987. Evolution of Chromium Ore Fields. New York, Van Nostrand Reinhold, 340pp.

Sunder Raju, P.V, Hanski, E., Merkle, R.K.W., Taikina-aho, O., Mohanthy, S.K., 2009, Rare exotic mineral inclusions in chromitites from Bangur, Orissa, India. Current Science, 97, 998-999.

Tsuru, A., Walker, R., Kontinen, A., Peltonen, P., Hanski, E., 2000. Re-Os isotopic systematics of the 1.95 Ga Jormua Ophiolite Complex, northeastern Finland. Chemical Geology, 164, 123-141.

Vuollo, J., Liipo, J., Nykänen, V., Piirainen, T., Pekkarinen, L., Tuokko, I., Ekdahl, E., 1995, An early Proterozoic podiform chromitite in the Outokumpu Ophiolite complex, Finland. Economic Geology, 90, 445-452.

Walker, R.J., Morgan, J.W., Hanski, E.J., Smolkin, V.F., 1997. Re-Os systematics of early Proterozoic ferropicrites, Pechenga Complex, Russia evidence for ancient 187Os enriched plumes. Geochimica et Cosmochimica Acta, 61, 3145-3160.

Walker, R.J., Prichard, H.M., Ishiwatari, A., Pimentel, M., 2002. The osmium isotopic composition of convecting upper mantle deduced from ophiolite chromites. Geochimica et Cosmochimica Acta, 66, 329-345

Zaccarini, F., Stumpfl, E.F., Garuti, G., 2004. Zr-Th-U minerals in chromitites of the Finero complex, Western Alps, Italy. evidence for carbonatite type metasomatism in a subcontinental mantle plume. Canadian Mineralogist, 42, 1825-1845.

Zaccarini, F., Garuti, G., Martin, R.F., 2006, Exotic accessory minerals in layered chromitites of Compo Formoso Complex, (Brazil). Geologica Acta, 4, 461-469.

Manuscript received March 2015;
revision accepted July 2015;
published Online October 2015.